Jurnal Kejuruteraan 34(4) 2022: 703-717
https://doi.org/10.17576/jkukm-2022-34(4)-18

Performance of Steel Perforated and Partially-Encased Composite Self-Connected Beams

Atyaf Abdul Azeez Maaroof, Jasim Ali Abdullah* & Suhaib Yahya Kasim

University of Mosul, College of Engineering, Civil Engineering Dept.

**Corresponding author: jassim24676@uomosul.edu.iq*

Received 2 November 2021, Received in revised form 14 November 2021
Accepted 14 December 2021, Available online 30 July 2022

ABSTRACT

The self-connected partially encased composite beams may be used rather than the conventional composite beams; those are connected by the concrete passing through the web-openings of the perforated profiles which works as shear connectors. This technique minimizes the construction cost and enhances the load carrying capacity and ductility of this kind of structures better than the perforated steel beams. The presented work investigates the performance of perforated steel and partially-encased composited self-connected simply supported beams applied to three-points of loading. The effect of the openings shape and the presence of concrete on the performance of the beams are investigated by testing eight specimens of perforated steel and composite beams. The openings' shapes of perforated steel profiles and composite beams were square, rectangular and circular. The solid steel profiles are taken as control beams in both exposed and encased specimens. The composite beam constructed using perforated steel profile with square openings was reinforced with conventional reinforcement, and setting its stirrups passing through the openings to improve the self connection. The failure modes, strain behaviours, and load-deflection curves were extensively discussed. The composite beams reinforced with perforated steel profiles exhibit higher composite performance than that reinforced with solid profiles. The concrete encasement improved the local deformation performance of the perforated steel profiles (50-300%), leading to a more ductile behaviour and a higher dissipation of energy. The square openings provide higher connectivity than other shapes due to the better arrangement of openings and presence of reinforced concrete.

Keywords: Perforated steel profiles; partially encased composite beam; self-connected; flexural performance; shear performance

INTRODUCTION

Self-connected partially encased composite beams can be described as composite beams constructed by casting plain or reinforced concrete inside perforated steel profiles. The concrete passed through the openings of the perforated web works as connectors, which eliminates the need for shear connectors that will reduce the construction cost. The performance of perforated steel and self-connected partially encased composite beams depends on the shape and arrangement of the web openings. Recently, composite members that constructed using steel profiles and plain or reinforced concrete have become essential parts of both bridges and commercial structures. Both materials steel and concrete behave as a unit when subjected to different type of loading. These types of structures gain their strength from the strength of both steel and concrete; that produces a highly economical and attractive structural system (Nardin & El debs 2009; Ali 2012). In 1922, encased beams were studied by the National Physical Laboratory tests in the report of filler joist panels (Adekola 1968). Many studies have conducted to investigate the performance of both fully and partially encased beams (Kindmann & Bergmann 1993; Roeder 1999; Hegger & Goralski 2006 and Elghazouli 2008).

Several studies investigated the behavior of the perforated steel beams with different shapes of web opening with plain concrete cast in the steel profiles to get a partially encased composite member. Liu and Chung (2003) developed a finite element model to investigate the effect of various large web openings shapes and sizes in perforated steel beams. The analysis revealed that the most crucial parameter in assessing the structural behavior of the perforated sections is the critical opening size. It was indicated that the depth of the openings controls the shear and moment resistance. It was reported that; plastic hinges always formed at both ends of the tee sections above and below the web openings at failure. All steel beams with large web openings of various shapes behave similarly under a wide range of applied moments and shear forces. Konstantinos and D'Mello (2012) conducted an experimental study to investigate the behavior of perforated steel beams subjected to high shear forces with different web opening. Test results proved that the stresses in the vicinity

of the web openings were affected by both inclination angles and opening size. The dimensions of the openings affect the deflections of the perforated beams. It was pointed out that the beams with vertical and inclined classic elliptical web openings behaved more effectively than beams with circular and hexagonal web openings, mainly in terms of stress distribution and local deflection.

Konstantinos et al. (2013) conducted an experimental and computational study of the vertical shear behavior of partially encased perforated steel beams. The study compared the behavior of conventional composite beams using perforated beams with that of the ultra shallow floor beam. It was also investigated the contribution of concrete in resisting the shear of partially encased perforated steel beams. The ultra shallow floor beams were tested with large circular web openings and the study showed that the concrete encasement enhanced the ultimate load-carrying capacity by up to 108%. In addition, Budi et al. (2017) used the finite element method (FEM) to study the effect of hexagonal web openings' size and the distance of castellated steel beams. The results of the comparative analysis were then verified by the experimental test of castellated steel beams. The tested specimens were fabricated from I-section with various hole angles of (45^o, 50^o, 55^o, 60^o, 65^o, and 70^o). The analysis showed that the capacity of specimens was doubled compared to the control specimen. Samer et al. (2018) conducted an experimental work to investigate the flexural performance of a new composite beam built-up of steel I-section, partially encased by concrete with different percentages of steel ratios with or without web openings. Six composite beams were tested with various ratios of steel. The tests were conducted by applying concentrated load at the mid-span of each specimen. The test results showed that the presence of web openings in the composite beams effectively enhances the flexural capacity and the energy absorption, and subsequently, the ductility increased. Satyarno et al. (2017) conducted an experimental study to investigate the behavior of full-height rectangular openings in steel beams with partially reinforced mortar encasement. The short span beams were used to study the shear failure mechanism, while the long span beams to study the flexural failure mechanism. It was concluded that the application of partial encasement in long-span specimens could prevent the Vierendeel mechanism and increase the yield moment capacity about 3.5 times of the original steel section yield moment.

Richard et al. (2017) performed a numerical study using ABAQUS software to investigate the behavior of simply supported composite castellated steel beams using a four-point load test. The castellated beams were fabricated with a hot rolled steel I- section. A composite solid steel beam was prepared as control specimen for comparison. The results showed that the load-carrying capacity of the composite castellated beams was enhanced to (6.24) times that of the solid section. In contrast, the composite solid beam is enhanced by (1.2) times the exposed solid specimen.

Hosseinpour (2018) conducted a push-out test with static loading to evaluate the ultimate shear capacity and ductility by testing different composite samples incorporating openings with various shapes. The test results were used to verify the developed FEM, which used to extend the parametric study. The results indicated that the samples with square openings have higher shear capacity than those with rectangular and circular shapes.

Sahar et al. (2019) theoretically studied the influence of web holes on the vertical deflection of castellated steel beams using the potential energy method and ANSYS software. The deflection was estimated depending on the shear resistance of castellated steel beams with various span lengths and flange breadths exposed to a uniform distributed load. The results showed that shear had a significant effect on the deflection of castellated steel beams, especially for medium and short-span beams. In addition, it was noticed that the influence of web shear on the deflection decreased as the castellated steel beam length increased. However, the difference between the analytical and numerical approaches did not exceed 6% for short beam length having narrow or wide sections.

Dai et al. (2020) presented a numeral model to simulate the behavior of composite slim-floor beams with various types of shear connectors including the reinforced concrete dowels. It was concluded that the dowel opening had an important role on load carrying capacity of this type of structure; where larger hole provides a higher shear capacity.

Kyriakopoulos et al. (2021) investigated the durability of composite slim-floor beams by testing seven simply supported specimens with various cross-sections subjected to concentrated load. The results showed that the flexural design of members was affected by the ductility and durability of beams. It is also revealed that the confinement of the concrete, and its influence on the performance of adopted specimens under large deformations.

Self-compacting concrete (SCC) was proposed in 1986(Okamura 1997), but the prototype was first developed in 1988 in Japan (Ozawa 1989). In 1998, the first international workshop on SCC was held in Kochi, Japan. Through efforts by Ozawa and his colleagues, more intensive research thrived, especially in large construction companies in Asia. Hence, SCC was used in many structures, including buildings, bridge towers, and bridge girders. Positive attributes of SCC include safety, reduced labor cost and construction time, and improved quality of the finished product (Okamura &Ouchi 1999, Marianne 1999 and Khayat et al 2000).

The composite structures with special construction conditions, such as the partially encased composite elements reinforced by perforated steel profiles, require the use of self-compacted concrete. Self-compacted concrete can be described as a high-performance material that can flow under its own weight, without external vibration, to attain consolidation by filling up formwork, even if slim openings between reinforcement bars constrain accessibility. This technology is a robust solution in the construction industry,

where mechanical vibration is not possible because of the complexity of formwork. Because of these advantages, investigations on SCC in civil engineering industry have become popular worldwide (Sallam 2013).

From prior studies it is noticed that there are no experimental studies have been investigated the performance of partially-encased composite beams with various shapes and arrangement of web-openings of the steel profiles and incorporating the SCC. Therefore, the goal of the current study is to investigate experimentally the performance of perforated steel and partially-encased composite beams with different shapes of web openings.

The main objective of this research is to suggest a novel arrangement of square openings for perforated steel and self-connected partially encased composite beams. It also aims to compare their performance with others constructed beams using perforated steel profiles with circular and rectangular shapes of openings. The tests were conducted by applying concentrated load acting at the mid-span of simply supported specimen. The experimental study consisted of three parts; the first part includes the investigation of the behavior of perforated steel beams with different shapes of openings. The second part includes studying the performance of partially encased composite beams reinforced with perforated steel profiles, same as those used in the first part. The third part incorporates comparing the performance of both exposed and partially encased specimens to investigate the effect of concrete presence.

EXPERIMENTAL PROGRAM

SPECIMENS PREPARATION

Rolled steel sections were used in this research (IPE 240). The grade of steel is ST 37.2 according to the specifications of (DIN 17100) (1980). The size of test specimens was (120×240 mm) and the yield strength is (fy=333.71 MPa). The dimensions and other details of the beams are illustrated in the Figure 1 and Table 1.

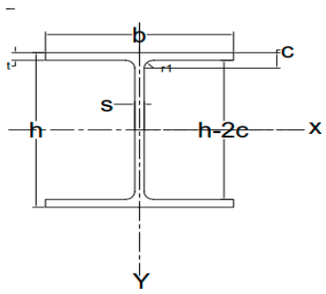

FIGURE 1. Rolled section details

TABLE 1. Dimensions and other details of beams

Sec. No.	Weight	Area	A_{web}	Dimensions						
				h	b	s	t	r1	C	h-2c
	(kg/m)	(cm^2)	(cm^2)	mm	mm	mm	mm	mm	mm	mm
240	30.70	39.10	13.66	240	120	6.2	9.8	15	24.8	190.4

Eight specimens have the same cross-sectional dimensions and spans were tested. These specimens were divided into two groups. The first group consisted of four specimens of perforated steel profiles without encasement; one is a solid steel beam as a control specimen and others with different shapes of web openings (circle, square, and rectangle), as shown in Table 2 and Figure 2. The second group consisted of four partially encased composite beams reinforced using the same perforated steel profiles as in the first group. The criteria of selecting the size of opening and spacing between them is the percentage of the cutting area was fixed as (43%) for all specimens which is taken from previous studies. To improve the self-connected, the stirrups of reinforced concrete was set passing through the square openings and tied to the longitudinal rebars. The reinforcement details of the composite specimen with suggested square web opening are shown in Figure 3. The yield strength of the reinforcing cage is (fy=463 MPa). The specimens were simply supported and the monotonic load was applied concentrically at the mid-span of each specimen.

TABLE 2. Details of experimental tested specimens.

Specimens	L mm	L_{eff} mm	f_{cu} MPa	f_y MPa
		Perforated Steel Beams		
Solid Steel Beam(SOSB)	2000	1900	----	333.71
Steel Beam with Square opening(SSB)	2000	1900	----	333.71
Steel Beam with Circular opening(CSB)	2000	1900	----	333.71
Steel Beam with Rectangular opening(RSB)	2000	1900	----	333.71

continue ...

... continued

	Composite Beams			
Composite Beam reinforced with Solid profile (SOCB)	2000	1900	36	333.71
Composite Beam reinforced with perforated steel profile with Square opening(SCB)	2000	1900	36	333.71
Composite Beam reinforced with perforated steel profile with Circular opening(CCB)	2000	1900	36	333.71
Composite Beam reinforced with perforated steel profile with Rectangular opening RCB	2000	1900	36	333.71

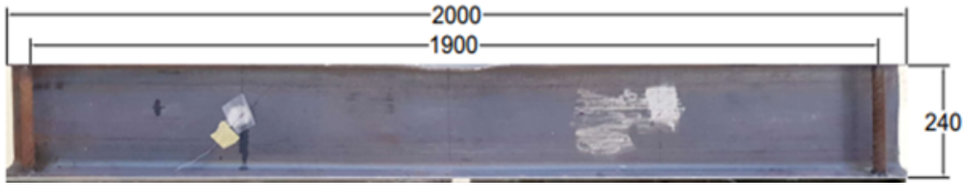

a) Solid Steel Beam(SOSB)

b) Steel Beam with Square opening(SSB)

c) Steel Beam with Circular opening(CSB)

d) Steel Beam with Rectangular opening(RSB)

FIGURE 2. Arrangement and dimension of web openings in the steel section (all dimensions are in mm)

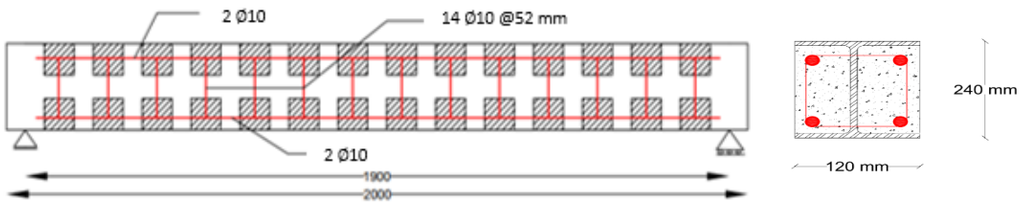

a) Suggested specimen b) Cross-Section of test specimen

FIGURE 3. Schematic of the test specimen(all dimensions are in mm)

Self-Compacted Concrete SCC is a special concrete that does not require vibration for placing and compaction. Therefore, the construction of the specimens in the current study needed this type of concrete due to shape of openings and presence of reinforcement. The mix was designed according to EFNARC (2005) and found that the content of cement 400 kg/m3, sand 990 kg/m3, gravel 810 kg/m3(the maximum aggregate size was 14 mm), limestone 75 kg/m3, water/cement ratio is 0.35, the dosage of super-plasticizer is 1% of the binder and the dosage of Poly Vinyl Acetate (PVA) 2 %.The above quantities were almost fixed except the water to cement ratio and the dosage of superplasticizer, were changed in many trials until arrived to the optimum quantities. Six standard cubes of (15×15×15 cm) were cast to test the compressive strength and six standard cylinders (15×30 cm) were cast to test the tensile strength. These cubes and cylinders were kept at the same conditions as the composite beams. The compressive and tensile strengths of concrete at 28 days were (fcu=36 MPa) and (ft=3.46 MPa), respectively. Figure 4 shows the casting of specimens using SCC.

TEST SETUP AND INSTRUMENTATION LAYOUT

The tests were conducted at the Construction Materials Lab. at the University of Mosul. The test setup as shown in Figure 5 consists of a rigid frame to support a vertical hydraulic actuator and a rigid beam to support the test specimens. The rigid beam is supported on the base of the rigid frame. The load was applied by using the (1500 kN) vertical actuator and the rigid frame. The supports were simply supported by adding a roller and hinge at the ends of the specimens. A thick bearing plate was utilized for loading to ensure uniformity of load distribution; and to prevent buckling at supports, (4 ϕ 25) bars welded between the two flanges at supports. Three Linear Variable Differential Transforms (LVDTs) were used to monitor the vertical displacement of the specimens at the bottom flange. One was placed at mid-span, while the others were placed at mid of half-span.

FIGURE 4. Casting of composite specimens using SCC

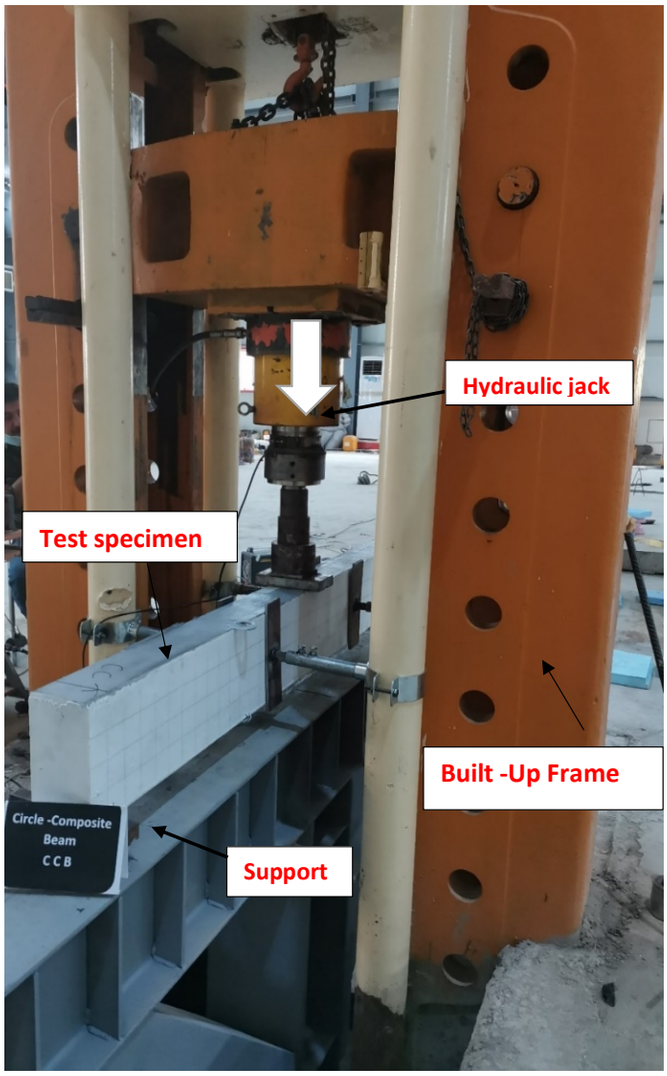

FIGURE5. Test setup for all specimens

To observe a primary mode of failure, web-post buckling and flange rolled buckling, uniaxial strain gauges were installed to monitor the deformations of steel web and flanges for both encased and without encasement specimens. As shown in Figure 6, each specimen was instrumented with strain gauges around the openings. Other longitudinal strain gauges were placed on the top and the bottom flanges to observe their axial deformations. For composite specimen (SCB), the behavior of the passed-through part of stirrups was monitored by four strain gauges set on two of them longitudinally.

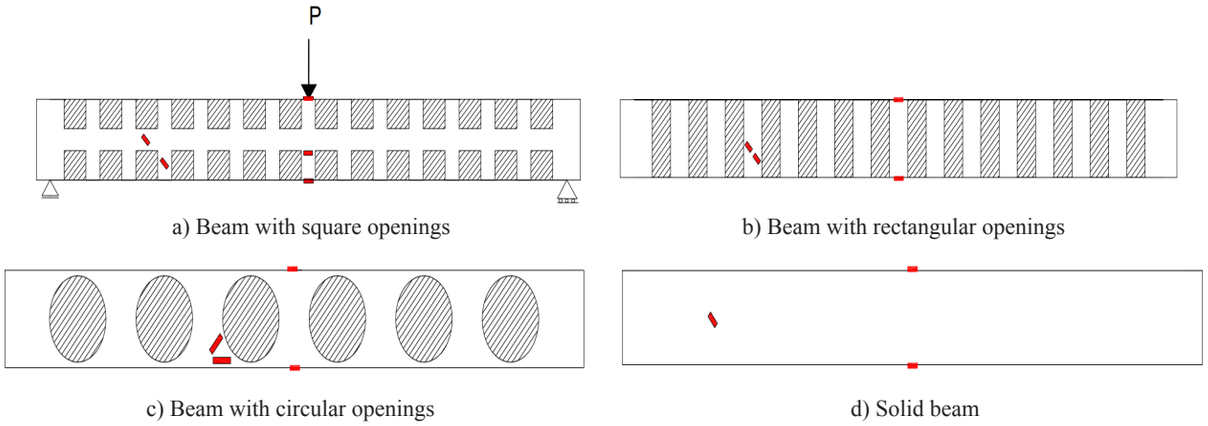

a) Beam with square openings

b) Beam with rectangular openings

c) Beam with circular openings

d) Solid beam

FIGURE 6. Position of strain gauges for each specimen

EXPERIMENTAL RESULTS AND DISCUSIONS

FAILURE MODES

Figure 7 shows the failure modes of the perforated steel beams. As shown in Figure 7(a), the web of the solid steel beam tended to buckle at (200 kN), which is about (85%) of the peak load. Local buckling took place near the mid-span and mid of the web while the top flange twisted beside the loading area. The use of the various shapes of openings causes special modes of failures in the perforated steel beams. Figure7 (b) shows the failure mode of the perforated steel beam with rectangular openings. The initial local buckling of web slices occurred at (113 kN), which is about (90%) of the peak load. The distortion warp of web slices happened between the load and one of the supports and seemed to be in (S) shape, while the top flange slightly twisted. The failure modes of perforated steel beams with circular and square openings are shown in Figure7(c & d). The local buckling of webs occurred when the applied load approached the peak load and at the mid-span and mid-height of the specimens, while the top flange twisted sharply near the loading area and slightly between the load and the supports.

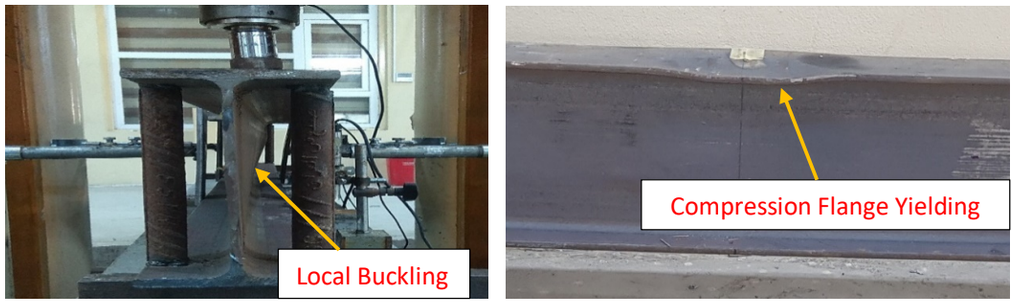

a) Local highly distorted web - flanges and web for SOSB

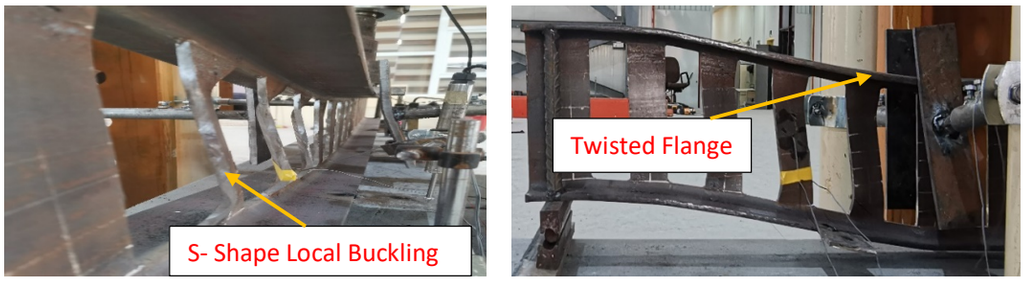

b) Local highly distorted web - flanges for RSB

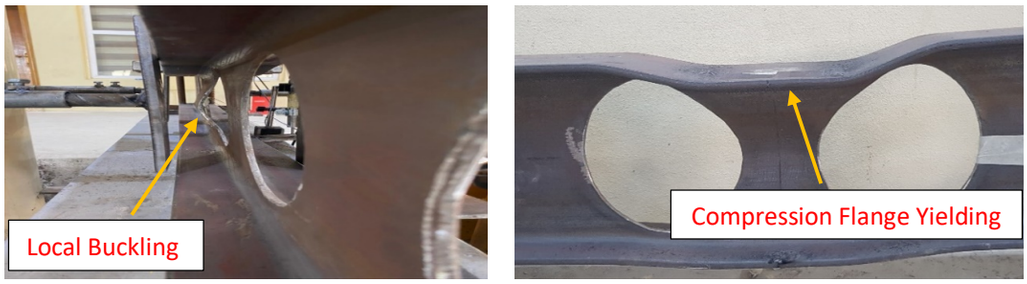

c) Local highly distorted web - flanges and web for CCB

d) Local highly distorted web - flanges and web for SSB

FIGURE 7. Failure mode for bare perforated steel beams

For composite beams, the compressive strength of concrete was (37.5 MPa) at testing time. The state before the initial cracking of concrete describes the linear behavior of composite beams monitored at testing time. The failure modes of partially encased composite specimens are shown in Figures 8 and 9. The first bending cracks appeared at (120, 100, 60, 40 kN) for SOCB, SCB, CCB, and RCB specimens, respectively. This variation shows that the stiffness of SOCB specimen is higher than the other specimens, while the stiffness of specimens reinforced with perforated steel beam depend on the arrangement of openings. The initial shear cracks of SOCB, SCB, CCB, and RCB specimens appeared at (140, 114, 70, and 62 kN), respectively. The composite specimen reinforced with a perforated steel profile with rectangular openings had smaller shear rigidity at the linear stage. The initial slipping between the concrete core and the flange took place at (265, 180, 170, and 41 kN) for SOCB, SCB, CCB, and RCB, respectively. When the concrete encasement of composite specimens was removed, the perforated web supported the composite action and showed no sign of local deformations. Accordingly, the failure occurred by high Vierendeel bending actions in the vicinity of the openings.

The perforated steel profiles showed slightly in-plane deformation compared to the non-composite perforated steel beams. At the same time, a slight local web buckling was observed on the diagonal line from the loading area to the supports, which implies a transfer of shear forces across the web openings after the concrete cracked. In contrast, loading was applied in the post-elastic region. The transfer of shear forces caused local bending moments and, therefore, limited local web buckling.

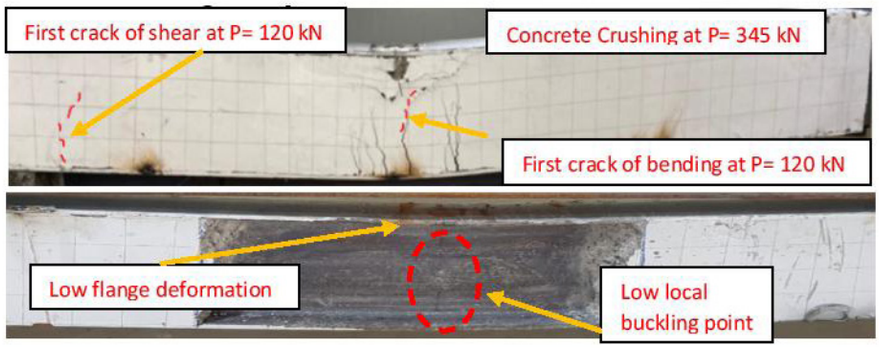

a) Crack pattern and failure mode for SOCB

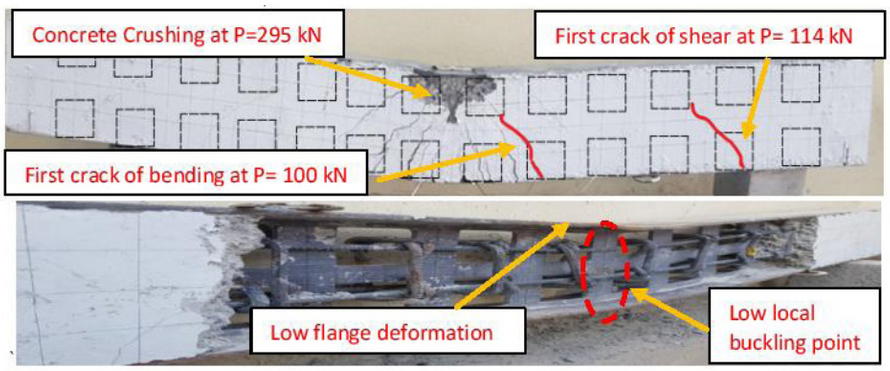

b) Crack pattern and failure mode for SCB

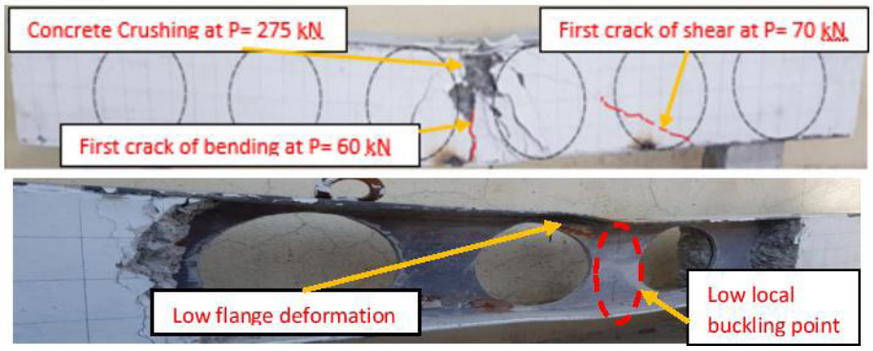

(c) Crack pattern and failure mode for CCB

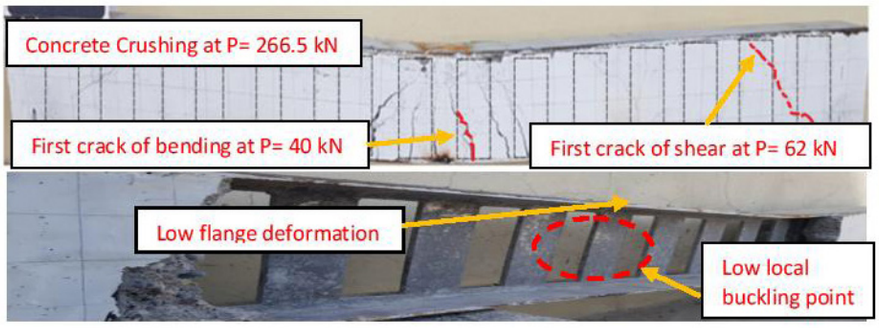

d) Crack pattern and failure mode for RCB

FIGURE 8. Crack and Failure modes for partially encased composite beam after removal of the damaged concrete

FIGURE 9. Load carrying capacity of the tested composite beams

TEST RESULTS AND BEHAVIORS

The test results provide information on the perforated steel and partially encased composite beams' elastic and plastic behavior with various web-opening shapes. The overall yielding happens at the web-post of all perforated steel specimens. The post-buckling of the web occurs at a load slightly more than that at which gross deformations are initially monitored. Finally, testing is stopped when the beam can withstand extra loading or is distorted. The load versus mid-span deflection curves of steel beams are shown in Figure 10. The solid steel beam has the higher load carrying capacity (237kN) compared to the perforated beams. The perforated steel specimens' load capacities depend on the arrangement of the openings. The RSB specimen load carrying capacity was lower than that of the other specimens due to removing the full height of the web when creating the rectangular openings. The figure also shows the difference in stiffness among perforated steel beams at the linear stage. The stiffness of specimens with circular openings is higher than that of the other specimens, although the cutting ratio for all perforated specimens was the same. The perforated beam with rectangular openings exhibits more energy dissipation than that of the others.

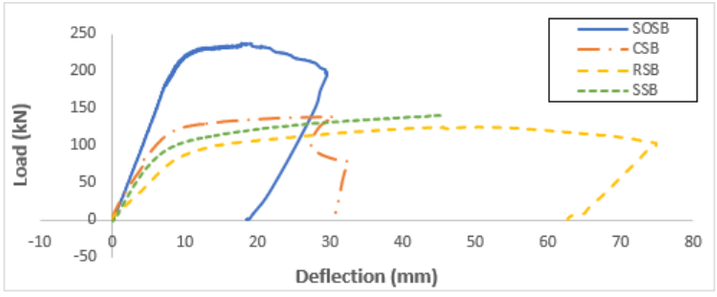

FIGURE 10. Load – Deflection curve for perforated steel beams

The behavior comparison diagrams of perforated steel and composite beams are illustrated in Figure 11. The figure shows that the composite beams exhibited better performance and higher load-carrying capacity than that of the perforated steel beams. The increase in the load-carrying capacity of composite specimens caused by the presence of concrete was (46, 110, 99, and 112%) for solid specimen and those with square, circle, and rectangular openings, respectively. These ratios indicate that the perforated beams exhibit higher composite action due to the presence of openings, which lead to bridging between both concrete, blocks, subsequently, the self-connection happens between them. The disparity among ratios can be attributed to the arrangement of openings, although the cutting ratio of the web is the same. Also, it was indicated that the specimens with square and rectangular openings have higher increase in load-carrying capacity due to the higher number and better arrangement of openings leading to an increase in the number of self-connecters.

One of the important reasons for the beams' capacities improvements is that the concrete restricted the web opening from buckling that occurred for the perforated steel beam. In addition, the interactions behavior that carried by the openings and the concrete.

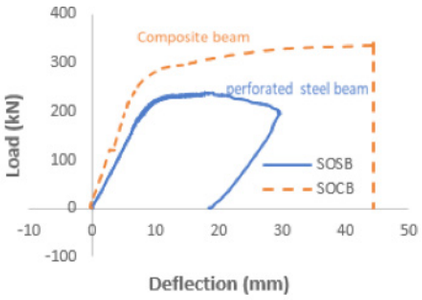

a) Load- deflection behavior for solid beam

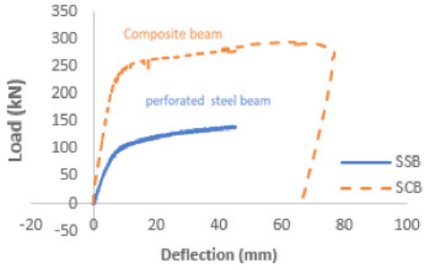

b) Load- deflection behavior for square holes

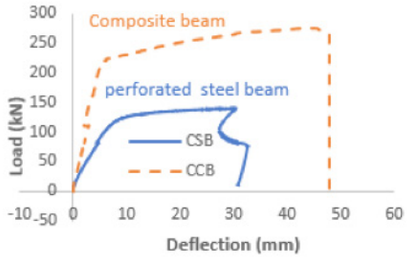

(c) Load- deflection behavior for circular holes

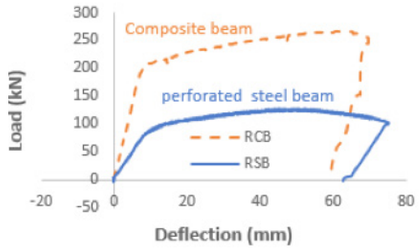

d) Load- deflection behavior for rectangular holes

FIGURE 11. Comparison of load-deflection behavior for the tested beams with and without concrete

Figure 12 shows the load-deflection curves of partially encased composite beams. Almost linear behavior is observed in all specimens' behavior up to around (200 kN). The composite beam reinforced with a solid profile exhibits a higher load-carrying capacity than other beams. The specimens reinforced with perforated profiles with rectangular and square openings behave more ductile due to higher deformation capacity and energy dissipation.

Figure13 shows the strain-load curves of top and bottom flanges for encased and without encasement beams. The strains of solid steel and composite beam reinforced with solid profile are illustrated in Figure13 (a). The figure indicates that the top and bottom flange yielded before the peak load and the top flange of the steel beam tends to be twisted. The top flange stilled to be compressed after the peak load until the failure that can be attributed to composite action and flexural mechanism. The strain of the bottom flange of the composite beam reinforced with the solid steel section was less than that of the solid specimen due to the composite action. Figs.13 (b,c, and d) show the relationship of the strain versus the applied load of perforated steel and composite specimens. The figures show that the top flange of all perforated steel beams did not yield at or before peak loads and tend to be twisted, while the bottom flange yielded before the peak loads. The strain of top and bottom flanges for encased specimens is significantly higher than those of without encasement specimens due to the composite action and flexural mechanism.

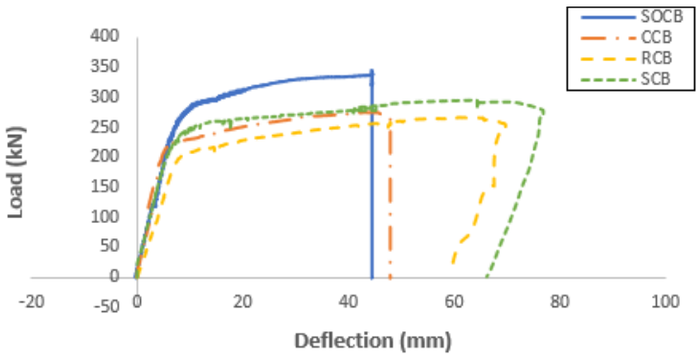

FIGURE 12. Load – Deflection curve for composite beams

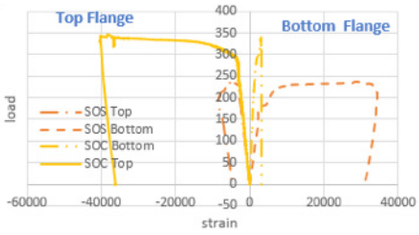

a) Behavior of top and bottom flange for solid beam

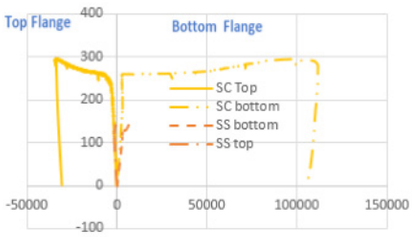

b) Behavior of top and bottom flange for square opening

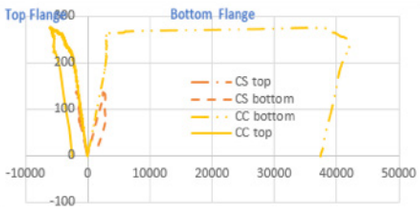

c) Behavior of top and bottom flange for circular opening

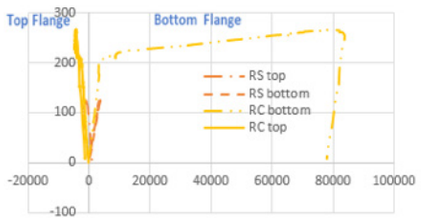

d) Behavior of top and bottom flange for rectangular opening

FIGURE 13. Strain behaviors of top and bottom flanges for steel perforated and composite beams

Figure 14 shows the relationship of strain of a stirrup vs. the applied load of the composite beam reinforced using perforated profile with square openings and steel cage. The stirrups exhibit better connection between the two blocks of concrete. The stress of stirrups reached (66%) of the yield strength that proofs the stirrups provide higher connectivity.

COMPARISON OF RESULTS

In this section, the effect of different structural parameters on the strength of specimens is illustrated. The strength comparisons of specimens are shown in Table 3. The cutting of the web by (43%) led to reduce the strength of perforated specimens more than (40 %) of the control beam (solid). The presence of concrete in the composite beams helps in minimizing the strength reduction to about (20%). Generally, the strength of composite beams was higher than that of non-cased. In contrast, the composite specimens reinforced with perforated steel profiles exhibited a higher load-carrying capacity ratio than that of non-cased by (100%) due to the self-connection that happened due to the presence of openings.

The shear failure mechanism is correlated to high shear forces acting on the beam. The formation of plastic hinges at the edges of the web openings or the corner of particular web openings deforms the tee sections above the web openings to a stretched shape. The effect of openings' shape is illustrated in Table 4 depending on the specimen perforated with rectangular openings as a control specimen because it's load carrying capacity was smaller than others. The table shows the ratio of the strength of perforated steel beams to the control specimen (P_u/P_u^R), which shows that the specimens perforated with circular and square openings exhibit higher load carrying capacity about (12%) due to the higher shear mechanism of both specimens. The flexural mechanism takes place under pure bending. The tee sections above and below the web openings are yielded in tension and compression until they become fully plastic. This mechanism happened with composite specimens reinforced with perforated steel profiles. Also, Table 4 shows the ratio of the strength of composite beams reinforced with perforated steel profiles to the control specimen which was perforated by rectangular openings has a lower load carrying capacity(P_u^C/P_u^{CR}).This ratio shows that the composite beam reinforced using steel profile perforated with square opening provide higher flexure mechanism.

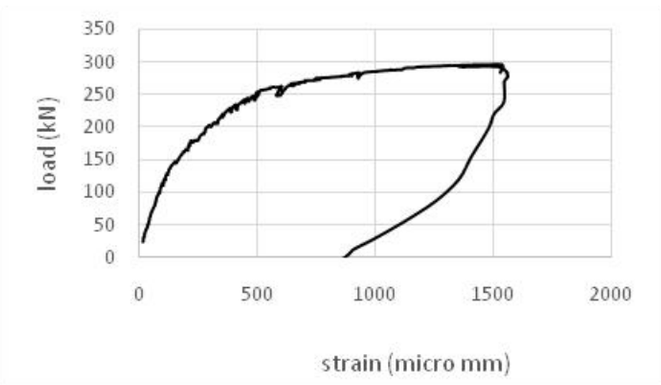

FIGURE 14. Strain of a stirrup of the SCB

TABLE 3. Strength comparisons of tested specimens

	P_U for steel (kN)	P_U for comp.(kN)	%minimized area of web	% Strength reduction of steel only	% Strength reduction of composite	% Strength enhancing (composite)
Solid	237.1	345.4	------	-----	------	45
Square	141.0	295.4	43	40.53	14.47	109.5
Circle	138.5	275.2	43	41.59	20.32	98.0
Rectangle	125.5	266.5	43	47.07	22.84	112.0

The yield and ultimate strengths of each specimen are identified and determined from the (P -Δ) curves, as shown in Table 5. The yield and ultimate strengths were defined from the standard procedure in reference (Park 1988), where P_y, $\boldsymbol{\Delta}_y$ are the yield load and displacement, while the P_u and $\boldsymbol{\Delta}_u$ are the ultimate load and displacement. Also, the table shows the ductility coefficient (μ) and the ultimate interstory drift ratio ($\boldsymbol{\theta}_u$)), which are defined as:

$$\mu = \frac{\Delta_u}{\Delta_y}$$

$$\theta_u = \frac{\Delta_u}{L}$$

Generally, all the perforated steel beams exhibited good deformation capacity. The table shows that the ductility coefficient and the ultimate inter-story drift ratio of perforated steel beams are greater than that of the solid specimen. The perforated specimen with square openings exhibits the highest ductility coefficient (5.21), while the ultimate inter-story drift ratio of specimen perforated with rectangular openings is the highest (5.33%).

As shown in Table 5, the composite specimens provide higher load carrying capacity and higher ductility than those of non-cased specimens. Also, the composite beam reinforced using perforated steel profile with square openings exhibits a higher ductility coefficient (7.25) and ultimate inter-story drift ratio (6.77%) than that of others due to the presence of reinforced concrete and better arrangement of openings.

CONCLUSIONS

The performance of perforated steel and partially encased composite self-connected beams was experimentally investigated. Eight specimens were tested and divided in two groups. The first group consisted of four specimens of perforated steel beams and the other group included four specimens of partially encased composite beams reinforced with the same profiles of the non-cased specimens. The specimens were tested as simply supported beams under a concentrated monotonic load at mid-span. The main parameters were the shape of web openings and the presence of concrete to get the composite action. The test results were analyzed extensively, and the following observations and findings can be listed:

1. From failure modes, it can be indicated that the perforated steel beams tend to buckle locally at or near the peak load, and the failure modes prove that the specimens failed as Veirendeel shear mechanism near or around the openings.
2. The presence of concrete in composite specimens reinforced with the perforated steel profiles keeps the web from local failure, and the concrete passing through the openings behaves as connectors.
3. For composite specimen reinforced with rebar cage and perforated steel profile with square opening, the stirrups exhibit better connection between the two blocks of concrete and The stress reached (66%) of the yield strength that proofs the higher connectivity.
4. The solid steel beam bears a higher load-carrying capacity than that of the perforated steel specimens, which varied depending on the shape and arrangement of the openings. The perforated specimen with rectangular openings exhibits lower bearing capacity than that of others due to the removing of full height of the web, which led to an increase in the area of plastic hinges occurring and failure mechanism.
5. The perforated steel and the other composite specimens reinforced with the same profiles exhibit higher deformation capacity and dissipation of energy.
6. The top and bottom flanges of the solid steel beam yielded before the peak load, while those of the perforated steel beams didn't yield.
7. The strain of top and bottom flanges for composite specimens is significantly higher than that of perforated steel specimens due to the composite action and flexural mechanism.
8. The strength of composite beams was higher than that of non-cased. In contrast, the composite specimens reinforced with perforated steel profiles exhibited a higher load-carrying capacity than that of non-cased by (100%) due to the self-connection that happened by the presence of openings.
9. The ductility coefficient and the ultimate interstory drift ratio of perforated steel beams were more significant than that of the solid specimen. The perforated specimen with square openings exhibited the highest ductility coefficient (5.44), while the ultimate interstory drift ratio of specimen perforated with rectangular openings was the highest (5.33%).

TABLE 4. Comparison of load carrying capacity of specimens against specimens with rectangular openings

Opening's shape	P_u(kN)	P_{uC}(kN)	P_u/P_{uR}	P_{uC}/P_{uRC}
Square	141	295.4	1.12	1.11
Circle	138.5	275.2	1.10	1.03
Rectangle	125.5	266.5	1	1

TABLE 5. Yield, ultimate and ductility of the tested beams

Specimen	Perforated steel				Composite beam			
	SOSB	SSB	CSB	RSB	SOCB	SCB	CCB	RCB
P_y(kN)	225.6	101.2	124.4	94.3	269.8	238.4	224.8	208.5
Δ_y (mm)	11.01	8.67	9.77	11.72	8.55	8.73	8.10	9.81
P_u(kN)	237.1	141.0	138.5	125.5	345.4	295.4	275.2	266.5
Δ_u (mm)	19.20	45.17	30.26	50.67	44.44	63.26	43.13	62.91
μ	1.74	5.21	3.09	4.32	5.20	7.25	5.33	6.41
θ_u (%)	2.02	4.75	3.19	5.33	4.68	6.77	4.54	6.62

ACKNOWLEDGEMENT

The authors would like to express their gratitude to the Dean of the College of Engineering and the Head of Civil Engineering Department at University of Mosul for their encouragement. The deepest gratitude is to Mr. Nazar Al-Sarraj, Dr Sameer Yasso, Dr Ali Natheer and the staff of Constructional Materials Lab in the University of Mosul for their assistant to complete this study.

DECLARATION OF COMPETING INTEREST

None

REFERENCES

Adekola, A.O.1968. Elastic and plastic behavior of cased beams. *Build. Sci*. (2): 321-330.

Ahmad, S. Masri, A. & Abou Saleh, Z. 2018. Analytical and experimental investigation on the flexural behavior of partially encased composite beams. *Alexandria Engineering Journal* 57(3): 1693-1712.

Ali, A. A. Sadik, S. N. & Abdul-Sahib, W.S. 2012. Strength and ductility of concrete encased composite beams. *Engineering and Technology Journal* 30(15): 2701-2714.

Budi, L. ukamta, S. &PartonoW.2017. Optimization of size and distance of Hexagonal hole in Castellated steel beams. *Procedia Engineering* (171):1092-1099.

Dai, X. Lam, D. Sheehan, T. Yang, J. & Zhou, K. 2020. Effect of dowel shear connector on performance of slim-floor composite shear beams. *Journal of Constructional Steel Research* 173:106243.

DIN 17100.1980. Steels for General Structural Purposes. *Deutsches Institut fur Normung E. V*.

EFNARC, 2005. *The European Guidelines for Self-Compacting Concrete Specification, Production and Use*: 1-68.

Elaiwi, S. Kim, B. & Li, L. 2019. Bending analysis of castellated beams. *Athens Journal of Technology& Engineering* 6(1): 1-16.

Elghazouli, A. Y. & Treadway, J. 2008. Inelastic behavior of composite members under combined bending andaxial loading. *Journal of Constructional Steel Research* (64):1008–1019.

Frans, R. Parung, H. Muhiddin, A. B. & Irmawaty, R. 2017. Finite element modelling of composite castellated beam. *In MATEC Web of Conferences*. (Vol. 138, p. 02009). EDP Sciences.

Hegger, J. & Goralski, C. 2006. Structural behavior of partially concrete encased composite sections with high strength concrete. *Composite Construction Insteel and Concrete*: 346-355.

Hosseinpour, E., Baharom, S., Badaruzzaman, W.H.W. & Al Zand, A.W., 2018. Push-out test on the web opening shear connector for a slim-floor steel beam: Experimental and analytical study. *Engineering Structures* 163: 137-152.

Khayat, K. H., Bickley, J. &Lessard, M. 2000. Performance of self-consolidating concrete for casting basement and foundation walls. *Materials Journal* 97(3): 374-380.

Kindmann, R. & Bergmann, R. 1993. Effect of reinforced concrete between the flanges of the steel profile of partially encased composite beams.*J. Construct Steel Research* (27):107-122.

Kyriakopoulos, P. Peltonen, S. Vayas, I. Spyrakos, C. & Leskela, M.V. 2021. Experimental and numerical investigation of the flexural behavior of shallow floor composite beams. *Engineering Structures* 231:111734.

Liu, T.C.H. & Chung, K.F. 2003. Steel beams with large web openings of various shapes and sizes: finite element investigation. *Journal of Constructional Steel Research* 59(9): 1159-1176.

Marianne, G. 1999. Self-compacting concrete: Industrialised site cast concrete*. In Proceedings of the First International RILEM Symposium. Swedish Cement and Concrete Research Institute Stockholm*: 651-658.

Nardin, S. D. & El-debs, A. L. H. 2009. Study of partially encased composite beams with innovative position of stud bolts. *J. Constr. Steel Res*. (65): 342-350.

Okamura, H. & Ouchi, M. 1999. Self-compacting concrete. Development, present use and future, self-compacting concrete. *Proceedings of the First International RILEM Symposium. Cachan Cedex, France: RILEM Publications:* 3-14.

Okamura, H. 1997. Self-compacting high-performance concrete. *Concrete International*. 19(7): 50-54.

Ozawa, K. 1989. High-performance concrete based on the durability design of concrete structures. *Proc. of the Second East Asia-Pacific Conference on Structural Engineering and Construction* (1): 445-450.

Park, R. 1988. Ductility evaluation from laboratory and analytical testing. *In Proceedings of the 9th world conference on earthquake engineering*, Tokyo-Kyoto, Japan (Vol. 8): 605-616.

Roeder, C.W. Chmielowski, R. & Brown, C. B. 1999. Shear connector requirements for embedded steel sections. *ASCE Journal of Structural Engineering* 125(2): 142-151.

Sallam, H. E. Badawy, A. A. & El-Emam, H. M. 2013. Numerical simulation of the performance of strengthened RC beams using smeared crack approach. *Journal of Jazan University-Applied Sciences Branch* 2(2): 30-44.

Satyarno, I. & Sulistyo, D. 2017. Full height rectangular opening castellated steel beam partially encased in reinforced mortar. *Procedia Engineering* (171): 176-184.

Tsavdaridis, K. D. & D'Mello, C. 2012. Optimisation of novel elliptically-based web opening shapes of perforated steel beams. *Journal of Constructional Steel Research* (76): 39-53.

Tsavdaridis, K. D. D'Mello, C. & Huo, B. Y.2013. Experimental and computational study of the vertical shear behavior of partially encased perforated steel beams. *Engineering Structures* (56): 805-822.